Low-lying levels in ^{59}Cr: Inadequacy of the *fp* model space and onset of deformation

S. J. Freeman,[1,2,*] R. V. F. Janssens,[2] B. A. Brown,[3] M. P. Carpenter,[2] S. M. Fischer,[2,4] N. J. Hammond,[2] M. Honma,[5] T. Lauritsen,[2] C. J. Lister,[2] T. L. Khoo,[2] G. Mukherjee,[2] D. Seweryniak,[2] J. F. Smith,[1] B. J. Varley,[1] M. Whitehead,[1] and S. Zhu[6]

[1]*Schuster Laboratory, University of Manchester, Manchester M13 9PL, United Kingdom*

[2]*Argonne National Laboratory, Argonne, Illinois 60439, USA*

[3]*National Superconducting Cyclotron Laboratory and Department of Physics and Astronomy, Michigan State University, East Lansing, Michigan 48824, USA*

[4]*DePaul University, Chicago, Illinois 60604, USA*

[5]*Center for Mathematical Sciences, University of Aizu, Tsuruga, Ikki-machi, Aizu-Wakamatsu, Fukushima 965-8580, Japan*

[6]*University of Notre Dame, Notre Dame, Indiana 46556, USA*

(Received 3 March 2004; published 1 June 2004)

The low-lying levels in ^{59}Cr have been studied with the ^{13}C(^{48}Ca,$2p$) reaction at a beam energy of 130 MeV. Data on ^{59}Mn, produced via the *pn*-evaporation channel, have set limits on the spin of the ground state in ^{59}Cr and enabled some spin-parity assignments of excited states to be made. The structure obtained in this study is clearly inconsistent with results of shell-model calculations within the full *fp* shell and requires inclusion of the $\nu g_{9/2}$ orbital. The sequence of states is understood within Nilsson model calculations assuming a moderate oblate ground-state deformation.

DOI: 10.1103/PhysRevC.69.064301 PACS number(s): 23.20.Lv, 27.50.+e, 21.60.Cs

I. INTRODUCTION

The region bounded by $N=28-40$ and $Z=20-28$ is of particular interest in the development of the shell model in neutron-rich systems. Application of the shell-model approach to regions far from stability requires calculations within novel model spaces, and effective interactions within these spaces must be developed. The full $\pi f_{7/2}\nu fp$ model space is small enough for large-scale calculations to be performed; new effective interactions have been developed recently [1]. These interactions have had some success in descriptions of low-lying excited states in neutron-rich *fp*-shell nuclei near $N=28$. For example, an $N=32$ subshell closure between the $\nu p_{1/2}$ and $\nu p_{3/2}$ orbitals has been observed which diminishes with increasing Z. Calculations using the new *fp*-shell interaction [2,3] have reproduced this effect reasonably well, which involves an increasing $\pi f_{7/2}-\nu f_{5/2}$ interaction as the $\pi f_{7/2}$ fills, shifting the $\nu f_{5/2}$ orbital to lower energies, thus closing the $N=32$ gap. Knowledge of excited states has, so far, been unavailable for the midshell region, and the effective interaction and the extent of the applicability of the model space have not been tested extensively. In fact, predictions [1] of a similar subshell gap at $N=34$ in the Ti isotopes do not appear to be substantiated by recent experimental measurements [4].

The success of this particular model space depends sensitively on an important structural issue: the strength of the $N=40$ subshell gap. Even at $Z=28$, the size of this gap is not clear, and the interpretation of the current data concerning the double-magicity of ^{68}Ni is the subject of debate [5,6]. The strength of a shell closure depends on both the energetic size of the gap and on the possible ways of generating excitations across it. A large gap will effectively isolate the low-lying nuclear structure in this region from the $g_{9/2}$ orbital, whereas a weak closure will facilitate excitations involving $g_{9/2}$ neutrons. Such excitations introduce the possibility of generating deformation, since the energy of the extreme m substates of the $g_{9/2}$ orbital varies strongly with the shape of the nucleus. This scenario would present challenges for the shell model in terms of the necessity to enlarge the model space and to develop an effective interaction within it.

The chromium isotopes lie in the middle of the $f_{7/2}$ proton shell. Those isotopes with neutron numbers near the middle of the shell would therefore naively be expected to show the greatest collective effects in this region. In fact, recent spectroscopic measurements following the β decay of ^{60,62}V produced in fragmentation reactions have observed γ-ray transitions at 646 and 446 keV in ^{60,62}Cr [7]. On the assumption that these correspond to transitions from the 2_1^+ states, and applying simple empirical systematics, the authors of Ref. [7] argue that these isotopes are strongly deformed with $\beta_2 \sim 0.3$. It is clear that evidence beyond a single γ-ray transition would be necessary to substantiate this speculation. The current project was therefore undertaken to study the low-lying level structure of ^{59}Cr. A spectroscopic investigation of such an odd-N nucleus yields information on the energies of the low-lying states, which is based predominantly on single-particle orbits. This can be used to test shell-model calculations within the *fp* basis, in addition to enabling some assessment of the influence of deformation on low-lying nuclear structure in this region.

Projectile fragmentation provides a production mechanism which allows the study of γ rays emitted after the β decay of neutron-rich fragments, but the currently available beam currents often limit such studies to singles γ-ray measurements of a small number of transitions. Significant invasion into the most neutron-rich regions requires detailed studies of deep inelastic and multinucleon transfer reactions.

*Electronic address: sjf@mags.ph.man.ac.uk

New experimental facilities are currently being developed for this purpose, and some pioneering measurements have already been carried out [8,9]. Smaller steps can be made using fusion reactions with the most neutron-rich projectiles and targets, where multiple charged-particle evaporation leads to a large excess of neutrons in the final system. In this work, the ^{13}C(^{48}Ca,$2p$) reaction has been used and multiple charged-particle evaporation has been isolated for the first time in the neutron-rich fp-shell nuclei. Electromagnetic radiation from this channel has been observed and new transitions have been associated with ^{59}Cr. Evidence, lacking in previous studies [10,11], is presented for a detailed low-lying level scheme, and some spin assignments are proposed.

II. EXPERIMENT

The reaction used here involves the fusion of ^{48}Ca projectiles with ^{13}C target nuclei to produce a neutron-rich compound system and, consequently, the prolific evaporation channels involve neutron emission. These channels have been studied previously using $\gamma\gamma$ coincidences with small numbers of detectors and without channel selection [12–16], but extensive excitation functions were carried out to help identify different products [12]. These were used here to estimate the best bombarding energy for production of the $2p$ channel. At the resulting energy, 130 MeV, evaporation codes [17] indicate that the dominating channels ($3n/4n$) have cross sections of the order of 100 mb. The strongest two-particle channels, $2n$ and pn, are produced at the millibarn level, the former being attenuated by the fusion barrier. No reliable estimate could be calculated for the $2p$ channel, suggesting a submillibarn cross section. Selective techniques are therefore necessary to extract events of interest from the stronger reaction channels. Measurements of recoiling nuclei from fusion reactions have been made extensively on the neutron-deficient side of stability, where recoil-mass separators are used to tag prompt γ-ray events with the arrival of particular ion groups at the focal plane. In general, the most neutron-deficient nucleus has the highest atomic number of those produced in the reaction, and the corresponding ion group is easily isolated from others in terms of its energy-loss characteristics in a suitable ion chamber. On the neutron-rich side of stability, the group of interest is generally sandwiched between scattered beam and the recoil-ion group with one Z higher, making ion-chamber performance and scattered beam reduction more important issues.

A ^{48}Ca^{11+} ion beam was generated in an ECR ion source and accelerated to 130 MeV using the ATLAS Superconducting Linear Accelerator at Argonne National Laboratory. It was used to bombard a 90-μgcm^{-2}-thick self-supporting ^{13}C target, isotopically enriched to 90%. The main contaminant in the target was ^{12}C. Prompt electromagnetic radiation was detected in the Gammasphere array [18] which, at the time of the experiment, consisted of 93 Compton-suppressed germanium detectors arranged in 15 rings around the beam direction. The overall photopeak efficiency was measured to be 9.8(2)% at a γ-ray energy of 1332.5 keV. 52 of these detectors were of a type with the outer electrode segmented into two halves. These detectors were arranged in the rings around 90° to the beam direction, and signals from the outer contacts were used to effectively narrow the opening angle of each detector, reducing the effects of Doppler broadening.

Ions recoiling from the target position were separated from primary beam particles and dispersed along the focal plane in terms of their mass-to-charge (A/q) ratio using the Fragment Mass Analyzer (FMA) [19]. The elements of the FMA were adjusted to optimize the transmission of ions with mass 59 and charge state 17^+, recoiling with an energy of 94.7 MeV. This charge state was found to give the largest yield of $A=59$ recoils, while minimizing the intensity of scattered beam particles at the focal plane. Scattered beam was further reduced by introducing slits at the exit of the first electric dipole element of the FMA to block the transmission of higher energy particles without affecting the yield of $A=59$ residues. Under these conditions, residues from prolific pure neutron-evaporation channels were also transported to the nominal focal plane of the FMA. Slits were introduced in front of the focal plane to exclude these intense groups which lie away from the central A/q value. A parallel-grid avalanche counter (PGAC) located at the focal plane enabled the horizontal and vertical positions of the ions to be measured. A fast signal from the anode of this detector was used to generate timing signals. Behind the PGAC, a segmented ion chamber measured the energy-loss characteristics of the recoiling ions. This detector was similar in design to that described in Ref. [20], except that the anode was segmented into three electrodes; two were 5 cm in length, followed by a third which was 20 cm long. The energy deposited under each anode was recorded separately. The ion chamber was filled with isobutane gas and operated at a pressure of 20 Torr, ensuring that the recoils of interest stopped under the third segment.

The data acquisition was triggered by an event corresponding to the arrival of an ion at the focal plane in coincidence with the detection of at least one γ ray in Gammasphere. Individual germanium times were recorded along with the time of the PGAC anode signal, both relative to the linac rf signal. Events were labeled with a time relative to the beginning to the experiment using a MHz scalar. Data were recorded under these conditions for a total of 57.5 h.

III. DATA REDUCTION AND ANALYSIS

Initially in the offline analysis, the germanium detectors were gain matched and calibrated using ^{243}Am and ^{152}Eu sources. A relative efficiency curve was produced from the same data. Doppler-shift corrections were made using a recoil velocity of $\beta=v/c=5.8\%$, which was extracted empirically.

In order to optimize the energy-loss information from the ion chamber, several software modifications were applied. Small gain drifts in the three energy-loss signals were corrected and a total recoil-energy signal, E, was formed from their sum. In order to assess the energy-loss characteristics of the ions, the signal from the first segment of the anode was plotted against the total recoil energy. A transformation was applied to these data to linearize the dependence of the energy-loss signal on recoil energy [20]; the resulting modi-

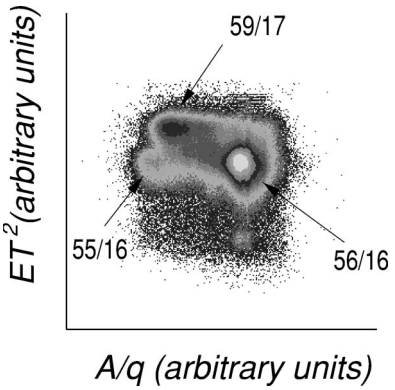

FIG. 1. Two-dimensional spectrum of charge-to-mass ratio, A/q, of ions at the focal plane of the FMA against the ET^2 parameter (see the text for details). Physical slits were used to restrict the extent of the focal plane and, therefore, the range of A/q values apparent in this figure. Similarly, the range of the ET^2 parameter is limited by software gates placed on both E and T during the analysis. Various ion groups in this spectrum are identified by their A/q ratios.

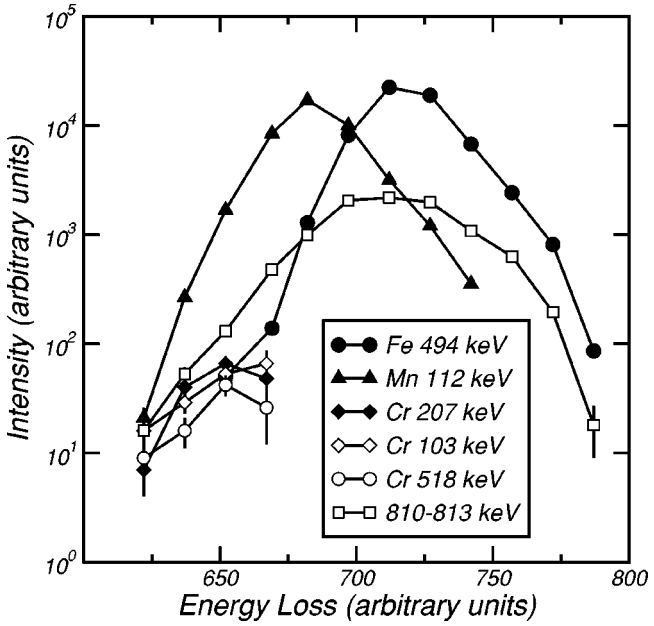

FIG. 2. The intensities of γ-ray transitions arising from recoiling $A=59$ ions, in spectra gated on different slices of the ion energy loss in the ionization chamber. The intensity is plotted against the centroid of each energy-loss slice.

fied parameter is referred to below as the energy loss, ΔE.

Tagging using a spectrometer which is dispersive in terms of the A/q ratio, can suffer from ambiguities as ions of different charge and mass may appear at the same position on the focal plane. In the current reaction, $^{59}Cr^{17+}$ recoils from $2p$ evaporation have an A/q ratio of 3.471. This is close to the ratio for $^{55}Cr^{16+}$ recoils from $\alpha 2n$ evaporation, 3.438. By a suitable manipulation of the time between PGAC and rf signals, a time-of-flight parameter, T, can be constructed for the recoiling ions. Combining this with the total recoil-energy signal in the form ET^2 produces a parameter proportional to the mass of the recoiling ion. This was used to resolve A/q ambiguities as illustrated in Fig. 1, where the ET^2 parameter is plotted against A/q. The $A/q=59/17$ and 55/16 ion groups clearly separate, allowing polygonal software gates to be applied. The identity of groups in this plot was confirmed by incrementing γ-ray energy spectra gated on the various ion groups. The γ-ray energy spectrum coincident with the $A/q=59/17$ group was dominated by known transitions in $A=59$ nuclei, mainly ^{59}Fe [13]. The $A/q=55/16$ ion group is coincident with known transitions in ^{55}Cr [14]. The 56/16 group shown in Fig. 1 arises from reactions on the ^{12}C contaminant in the target and is dominated by ^{56}Fe [21], the $4n$ evaporation channel. There is a continuous background of events underlying these ion groups which is coincident with known ^{57}Fe transitions [14]. These events are associated with tails from an intense group masked off by the focal-plane slits. A polygonal software gate was placed around the $A/q=59/17$ events to select them for subsequent analysis.

The energy-loss characteristics of the $A=59$ events were investigated by measuring intensities of γ-ray transitions in spectra gated on different ranges of the modified energy-loss parameter, ΔE. The results are shown in Fig. 2 for typical transitions in Mn and Fe nuclei, in addition to candidate lines in ^{59}Cr. Transitions with energies of 112 and 494 keV are strong, clean peaks which have been previously identified with ^{59}Mn [22] and ^{59}Fe [13], respectively. The 112-keV transition is one of only two known in ^{59}Mn from the β-decay studies of Ref. [22], and the $\gamma\gamma$ coincidences from the current data have allowed a significant extension of this level scheme [23]. The 112-keV transition is clearly associated with a lower energy loss than the 494-keV line; many other transitions which are coincident with the 112-keV line exhibit a similar behavior. Also shown are a number of transitions which have lower energy losses than the 112-keV line. These are candidates for transitions in ^{59}Cr. There is also a multiplet of lines in the spectrum at energies between 810 and 813 keV which appears to have an unusual energy-loss spectrum as shown in Fig. 2; a transition within this energy range appears to be present in all three mass-59 isobars. In Fig. 3(a), a γ-ray spectrum is shown which is in coincidence with $A=59$ recoils with a gate on energy losses covering the mean energy loss expected for Cr isotopes, corresponding to a slice in Fig. 2 centered on channel 652. Figure 3(b) presents a similar spectrum for the next energy-loss slice down, centered on channel 637 in Fig. 2. The candidate ^{59}Cr lines clearly persist in the lower ΔE spectrum, while lines associated with ^{59}Mn fall off in intensity more quickly. Of particular interest is the area of the spectrum around 813 keV. Analysis of the level scheme of ^{59}Mn from the current data (as discussed in Ref. [23]) indicates that an 812-keV transition lies above a line with energy of 720 keV. This 720-keV peak is clearly visible in Fig. 3(a) along with a group around 812 keV. In Fig. 3(b), the 720-keV transition has fallen dramatically in intensity, whereas a line at 813 keV persists. Closer inspection shows a shift in the centroid of the 812/813-keV group between these two spectra. An 813-keV transition is therefore associable with ^{59}Cr. The energies and relative intensities of transitions assigned to ^{59}Cr are listed in Table I.

The Cr fraction in the $A=59$ events was enhanced by placing a software gate on ΔE, corresponding to the lowest

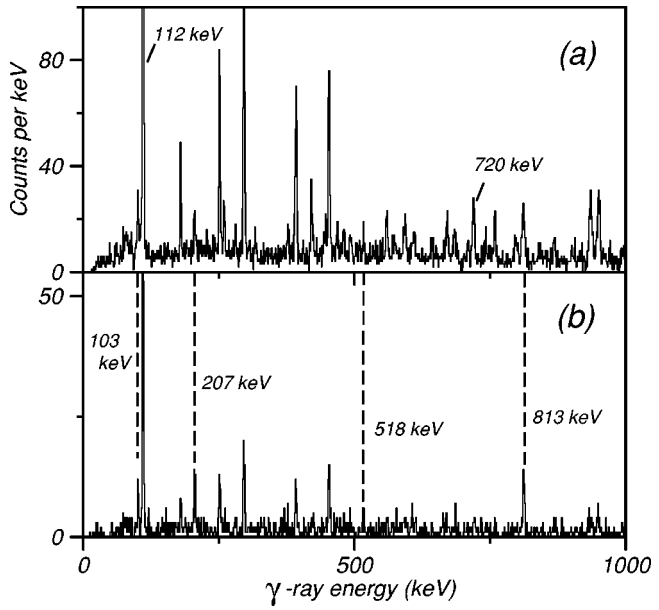

FIG. 3. Singles γ-ray energy spectra for $A=59$ events gated by different values of energy loss in the ion chamber. The energy-loss gate for spectrum (a) corresponds to the mean value for Cr ions. The spectrum in (b) is for a lower energy loss (see the text for details). Transitions associated with ^{59}Cr persist in spectrum (b), while the intensity of transitions from ^{59}Mn is reduced when comparing the two spectra. Transitions are labeled by their energies in keV.

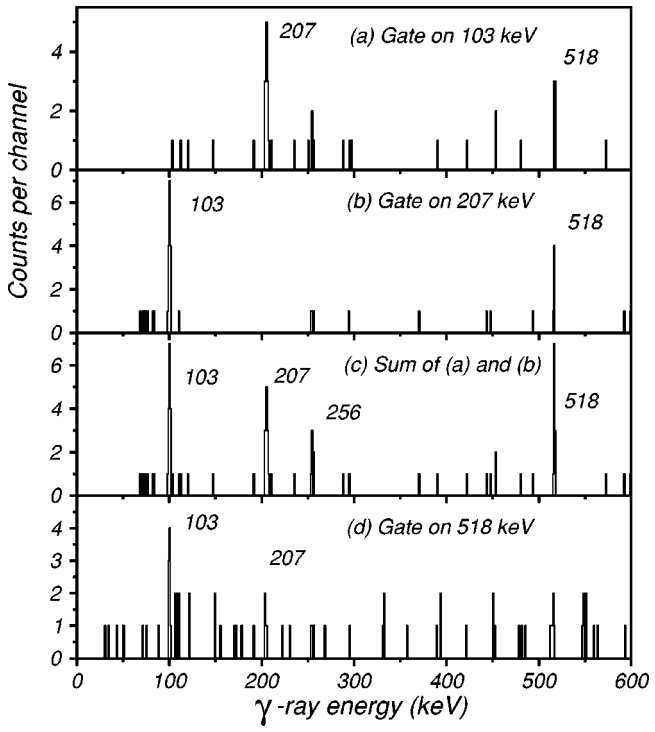

FIG. 4. γ-ray coincidence spectra for mass-59 events, with a condition on the energy-loss parameter to select Cr ions (see the text for details). The spectra are additionally gated on γ-ray energies of (a) 103 keV; (b) 207 keV; and (d) 518 keV. Spectrum (c) shows the sum of the 103- and 207-keV gates.

three slices in Fig. 2. From this subset of data, $\gamma\gamma$ events were extracted and used to produce the gated γ-ray energy spectra in Fig. 4. The 103-, 207-, and 518-keV transitions are clearly in coincidence, despite the scarcity of data. The sum of 103- and 207-keV gates also indicates the possibility of a further transition with an energy of 256 keV, although only a hint of this is seen in the 518-keV coincidence gate.

TABLE I. Energies and deduced spins of excited states in ^{59}Cr. Measured transition energies and relative intensities of deexciting γ rays are listed. Relative intensities of transitions have been corrected for efficiency and internal conversion. The decay of the state marked with an "a" was not observed in the current work as it has a long lifetime of 96(20) μs, but is included in the table for completeness with the transition energy adopted from Ref. [7].

Level energy (keV)	J^π	Transition energy (keV)	Relative intensity
0.0	(1/2)−		
102.7(2)	(3/2)−	102.7(2)	100
309.8(2)	(5/2)−	207.1(3)	82(19)
502.8(11)	(9/2+)	193(1)[a]	
827.8(4)	(13/2+)	518.0(2)	55(28)
1093.8(11)	(7/2)−	256(1)	19(13)
1316.0(11)	(9/2)−	813.2(3)	220(26)

[a]Isomeric decay not observed in the current experiment.

IV. RESULTS

There have been two previous studies of ^{59}Cr. Measurements of the decay of an isomer with a half-life of 96(20) μs, produced in projectile fragmentation [11], have established transitions with energies of 102, 193, and 208 keV (no uncertainties were quoted). A study of the β decay of ^{59}V [10] produced in a similar fashion observed only two transitions with energies of 102(1) keV and 208(1) keV. This established the 193-keV γ ray as directly deexciting the isomer. No evidence was presented to place the other two lines in a level scheme. The current work confirms the two low-energy transitions and establishes three new ones. On the basis of coincidence relationships, the level scheme shown in Fig. 5(a) was constructed. In addition, some information concerning spin-parities has also been obtained, as discussed below. The isomeric decay is not observed in the current experiment as its lifetime and the recoil velocity are such that the majority of the isomeric decays occurs after the recoils have left the fiducial volume of Gammasphere. Nevertheless, the 193-keV transition deexciting the isomer is included in Fig. 5(a) for completeness.

Care needs to be taken in handling the intensities of low-energy lines as their poor timing characteristics can lead to a loss of efficiency compared to that measured in singles γ-ray data with a radioactive source. The current intensities were extracted from an A/q-gated γ-ray spectrum without any timing gates placed on the individual germanium detectors, after first establishing that time-random background was not

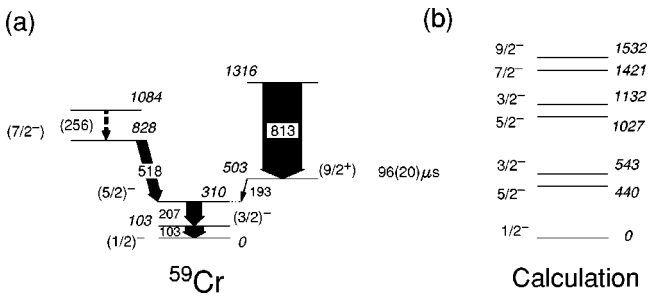

FIG. 5. Energies of levels in ^{59}Cr: (a) The level scheme deduced from the current work, with the addition of the 193-keV isomeric decay from Ref. [11]. The levels are labeled by their spin-parity and excitation energy. The widths of the arrows represent the relative intensity of the γ-ray transitions. The spin-parities for the states at 1084 and 1316 keV are tentatively $11/2^-$ and $13/2^+$, respectively; see the text for more details. (b) The level scheme from a shell-model calculation within the full *fp*-shell basis using the GXPF1 interaction [1].

an important issue. It was found that time gates result in a significant reduction of the efficiency for low-energy lines, whereas above ~180 keV the efficiency changed by less than 10%.

The 813-keV transition is not in coincidence with any of the other transitions in ^{59}Cr listed in Table I. It could feed directly into the ground state, bypassing the low-lying structure, but this is unlikely as yrast feeding is expected. It is, therefore, probable that this is a transition decaying to the 96-μs isomer from a state at an excitation energy of 1316 keV, as indicated in Fig 5(a). A search was made for transitions above the 1316-keV state in a spectrum gated on an energy of 813 keV. The only lines that were clearly visible were those associated with contaminating transitions in ^{59}Mn and ^{59}Fe, and no candidates were found with certainty for higher-lying transitions in ^{59}Cr. It is plausible that such transitions are of higher energy and thus appear too weakly in the gated spectrum to be observed.

The level of statistics for ^{59}Cr was insufficient to perform an angular distribution or correlation analysis. However, the spins of some of the states can be deduced, albeit in a less rigorous manner. Limits on the ground-state spin of ^{59}Cr can be established by combining previous measurements of the β decay of ^{59}Cr [22] with the information gained on ^{59}Mn from the present data. The β-decay studies observed two γ-ray transitions in ^{59}Mn with energies and relative intensities of 1239 keV (100%) and 112 keV (8%). Results for ^{59}Mn from the current data [23] indicate that the 112-keV transition has the highest intensity of all ^{59}Mn γ rays, and is placed as the lowest-lying transition. It has a measured angular distribution which is consistent with a stretched dipolar character. No in-beam γ ray with an energy of 1239 keV was observed, making it likely that it runs in parallel to the 112-keV transition and that it deexcites a non-yrast state populated in β decay, but not in fusion evaporation. The ground-state spin of ^{59}Mn has recently been firmly established as $5/2^-$[24], giving a first-excited state at an excitation energy of 112 keV with a spin of $7/2^-$ when combined with the current results. In order to reproduce the observed β-decay intensities, the ground-state spin of ^{59}Cr has to be less than $5/2^-$ or greater than $9/2^-$, otherwise the 112-keV transition would be fed by an allowed β-decay transition and would appear with much greater intensity than was measured in Ref. [22]. Given the available single-particle orbitals in this region, an assignment of $1/2^-$ or $3/2^-$ would be most likely.

Further limitations may be placed on the ground-state and low-lying state spins since no transition is observed with an energy of 309.8 keV running parallel to the 103- and 207-keV decay path, at least with an intensity greater than ~10% of that of the 207-keV line. The spin of the isomeric state, and the state fed by the 193-keV isomeric decay, have been previously assigned to be $9/2^+$ and $5/2^-$, respectively [11]. This assignment is based on a comparison of the measured lifetime of the isomer with that expected for an M2 single-particle transition, given the possible low-lying orbitals. If low-lying transitions are assumed to be limited to stretched M1 or E2 transitions, two alternative scenarios are possible for the decay of the state at 309.8 keV: two M1 transitions in series with an unobserved E2 γ ray in parallel ($5/2$–$3/2$–$1/2$ spin sequence); or an E2 decay followed by an M1 transition in series with an unobserved M1 γ ray in parallel ($5/2$–$1/2$–$3/2$ spin sequence). Taking typical values for reduced single-particle transition rates in $A=21$-44 nuclei (10 and 0.1 single-particle units for E2 and M1 transitions, respectively) [25], an upper limit may be deduced for the reduced transition probability for the unobserved parallel transition in each case. For the first scenario, the B(E2) for the 309.8-keV transition is less than ~60 single-particle units. The state at 309.8 keV would have a mean life of the order of ~30 ps under these assumptions. However, the B(M1) value for the 309.8-keV transition under the second scenario would be less than $\sim 7\times 10^{-6}$ single-particle units and therefore atypically retarded for this mass region. Additionally, the mean life of the 309.8-keV level would also be noticeably long, of the order of ~15 ns, inconsistent with experimental observation. The spin sequence, $5/2$–$3/2$–$1/2$, for the lowest-lying levels is therefore favored.

A similar argument for the 827.8-keV state based on the nonobservation of a 725-keV transition to the first-excited state turns out not to place any such restrictions; reasonable reduced transition probabilities are obtained for either $7/2$ or $9/2$ spin assignments, although yrast feeding arguments suggest the lower of the two values. Spins for the states at 1316 and 1084 keV are suggested to be $13/2^+$ and $11/2^-$, respectively, on the assumption of yrast feeding. The overall spin assignments are shown in Fig. 5(a).

V. INTERPRETATION

The low-lying structure of ^{59}Cr should reflect the single-neutron states at $N=35$ and, consequently, is expected to be dominated by single-neutron excitations involving $1f_{5/2}$, $2p_{1/2}$, and $2p_{3/2}$ orbitals, along with $1g_{9/2}$ state, depending on the strength of the $N=40$ closure. The β decay of $^{59}_{23}V_{36}$ [10] feeds the $5/2^-$ state at 309.8 keV, and possibly the $3/2^-$ state at 102.7 keV, which suggests an $f_{5/2}$ parentage for at least the $5/2^-$ state via allowed $\pi f_{7/2}\rightarrow\nu f_{5/2}$ β decays. Calculations have been performed within the full *fp*-shell basis using the GXFP1 interaction [1]. This interaction has been

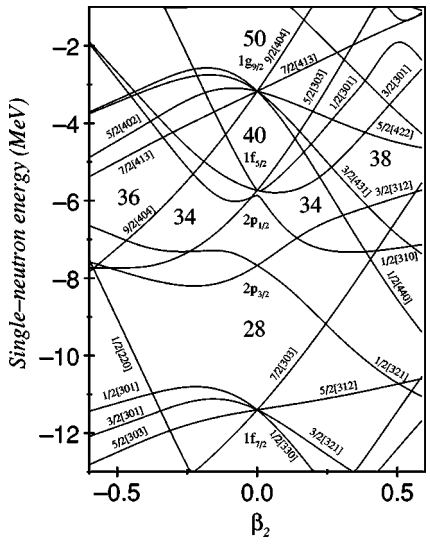

FIG. 6. Single-neutron energies for ^{59}Cr calculated in a Woods-Saxon potential with the universal parameter set from Ref. [26], as a function of deformation parameter β_2. Spherical single-particle orbitals are labeled by the usual nlj quantum numbers, and some significant gaps in the level structure are indicated by the appropriate neutron numbers. Asymptotic Nilsson quantum numbers are used to label individual states, where such a description is appropriate.

shown to be the best at reproducing the systematics of first-excited states in even-even neutron-rich isotopes near $N=32$ [2], although it gives general results similar to other effective interactions that have been used in this region [3]. The calculated GXFP1 energy levels are presented in Fig 5(b). Although the spin and parity of the ground state are reproduced, comparison with the experimental level scheme reveals a failure to provide an adequate description of the low-lying states; the experimental levels are differently ordered and compressed compared with the calculation. In addition, the low-lying $9/2^+$ state is very obviously outside of the fp-model space.

The observation of a $9/2^+$ state at an excitation energy of only 503 keV clearly demonstrates the necessity of including the $g_{9/2}$ orbital in the calculation. This requires the development of an effective interaction within the extended gfp space. Some insight may be gained into the structure of the low-lying states of ^{59}Cr by considering the energies of single-neutron orbitals near the Fermi surface. Figure 6 is the result of calculations within a Woods-Saxon potential using the universal parameters from Ref. [26]. For small oblate deformations, the $g_{9/2}$ orbital falls dramatically in energy towards the Fermi surface. A $1/2^-$ ground state of $2p_{1/2}$ spherical parentage is obtained for oblate ground-state shapes with $|\beta_2| \lesssim 0.25$. Prolate deformations are not consistent with the presence of a low-lying $9/2^+$ state, nor with a $1/2^-$ ground state. Within the range of deformation from $\beta_2=0$ to -0.25, low-lying states with spins $3/2^-$ and $5/2^-$ are easily generated by single-neutron excitations into states of $f_{5/2}$ spherical parentage, consistent with the observed low-lying states and the β decay feeding into them. Thus, the low-lying levels appear consistent with a moderate oblate ground-state deformation.

Such inferences from simple level sequences provide a qualitative insight, but reality is likely to be more complex. While the ground- and $9/2^+$ states may have oblate deformation to some extent, the presence of gaps at $N=34$ for both oblate and prolate shapes (see Fig. 6) suggests that shape coexistence may arise, or that levels with admixtures of oblate and prolate states may form the basis of many low-lying states. There is an interesting parallel here between the $A=60$ and $A=80$ regions; the neutron Fermi surface has a similar position in terms of single-particle orbitals to that for both types of nucleons in the $A=80$ region. In ^{72}Kr, for example, the large gap at $Z=N=36$ results in an oblate ground state, but low-level density on the prolate side conspires to produce a prolate 0^+ first-excited state [27]. Although the strong cooperative effects between protons and neutrons in the same orbitals is lacking in the $A=60$ region, similar phenomena may occur.

The transition feeding the isomer has an energy, 813.2(3) keV, similar to that observed for the $2^+ \rightarrow 0^+$ transition in ^{58}Cr with an energy of 880 keV [28]. It is interesting to speculate whether this is another example of the same weak coupling between the $g_{9/2}$ single-particle state and the core that has been observed in less neutron-rich systems [12]. However, a less tentative spin assignment for the state at 1316 keV would be needed to confirm this suggestion.

VI. CONCLUSION

In conclusion, two-proton evaporation from neutron-rich fp-shell compound nuclei has been observed for the first time in the fusion of a ^{48}Ca beam with a ^{13}C target. Coincident γ-ray measurements have established the sequence of low-lying levels, and arguments for spin assignments have been presented. This sequence is clearly inconsistent with shell-model calculations incorporating only the fp-model space and the influence of the $\nu g_{9/2}$ orbital is evident at low excitation energies. The observed structure appears consistent with a moderate oblate ground-state shape. There is clearly opportunity to study other nuclides in this region by two-proton evaporation channels.

ACKNOWLEDGMENTS

This work was supported by the U.K. Engineering and Physical Sciences Research Council (EPSRC), the U.S. Department of Energy, Office of Nuclear Physics, under Contract No. W-31-109-ENG-38, and the National Science Foundation under Grant No. PHY-0244453. M.W. acknowledges financial support from EPSRC.

[1] M. Honma, T. Otsuka, B. A. Brown, and T. Mizusaki, Phys. Rev. C **65**, 061301 (2002).
[2] J. I. Prisciandaro, P. F. Mantica, B. A. Brown, D. W. Anthony, M. W. Cooper, A. Garcia, D. E. Groh, A. Komives, W. Kumarasiri, P. A. Lofy, A. M. Oros-Peusquens, S. L. Tabor, and M. Wiedeking, Phys. Lett. B **510**, 17 (2001).
[3] R.V.F. Janssens, B. Fornal, P. F. Mantica, B. A. Brown, R. Broda, P. Bhattacharyya, M. P. Carpenter, M. Cinausero, P. J. Daly, A. D. Davies, T. Glasmacher, Z. W. Grabowski, D. E. Groh, M. Honma, F. G. Kondev, W. Królas, T. Lauritsen, S. N. Liddick, S. Lunardi, N. Marginean, T. Mizusaki, D. J. Morrissey, A. C. Morton, W. F. Mueller, T. Otsuka, T. Pawłat, D. Seweryniak, H. Schatz, A. Stolz, S. L. Tabor, C. A. Ur, G. Viesti, I. Wiedenhöver, and J. Wrzesiński, Phys. Lett. B **546**, 55 (2002).
[4] S. N. Liddick, P. F. Mantica, R.V.F. Janssens, R. Broda, B. A. Brown, M. P. Carpenter, B. Fornal, M. Honma, T. Mizusaki, A. C. Morton, W. F. Mueller, T. Otsuka, J. Pavan, A. Stolz, S. L. Tabor, B. E. Tomlin, and M. Wiedeking, Phys. Rev. Lett. **92**, 072502 (2004).
[5] K. Langanke, J. Terasaki, F. Nowacki, D. J. Dean, and W. Nazarewicz, Phys. Rev. C **67**, 044314 (2003).
[6] O. Sorlin, S. Leenhardt, C. Donzaud, J. Duprat, F. Azaiez, F. Nowacki, H. Grawe, Zs. Dombrádi, F. Amorini, A. Astier, D. Baiborodin, M. Belleguic, C. Borcea, C. Bourgeois, D. M. Cullen, Z. Dlouhy, E. Dragulescu, M. Górska, S. Grévy, D. Guillemaud-Mueller, G. Hagemann, B. Herskind, J. Kiener, R. Lemmon, M. Lewitowicz, S. M. Lukyanov, P. Mayet, F. de Oliveira Santos, D. Pantalica, Yu.-E. Penionzhkevich, F. Pougheon, A. Poves, N. Redon, M. G. Saint-Laurent, J. A. Scarpaci, G. Sletten, M. Stanoiu, O. Tarasov, and Ch. Theisen, Phys. Rev. Lett. **88**, 092501 (2002).
[7] O. Sorlin, C. Donzaud, F. Nowacki, J. C. Angélique, F. Azaiez, C. Bourgeois, V. Chiste, Z. Dlouhy, S. Grévy, D. Guillemaud-Mueller, F. Ibrahim, K.-L. Kratz, M. Lewitowicz, S. M. Lukyanov, J. Mrasek, Yu.-E. Penionzhkevich, F. de Oliveira Santos, B. Pfeiffer, F. Pougheon, A. Poves, M. G. Saint-Laurent, and M. Stanoiu, Eur. J. Phys. **16**, 55 (2003).
[8] W. Królas, R. Broda, B. Fornal, T. Pawłat, H. Grawe, K. H. Maier, M. Schramm, and R. Schubart, Nucl. Phys. **A724**, 289 (2003).
[9] B. Fornal, R. Broda, W. Królas, T. Pawłat, P. J. Daly, I. G. Bearden, Z. W. Grabowski, R. H. Maier, D. Nisius, L. Richter, M. Sferazza, M. Carpenter, R.V.F. Janssens, T. L. Khoo, T. Lauritsen, D. Bazzacco, S. Lunardi, C. Rossi Alvarez, G. De Angelis, P. Bednarczyk, K. H. Maier, and R. Schubart, Acta Phys. Pol. B **26**, 357 (1995).
[10] O. Sorlin, C. Donzaud, L. Axelsson, M. Belleguic, R. Béraud, C. Borcea, G. Canchel, E. Chabanat, J. M. Daugas, A. Emsallem, M. Girod, D. Guillemaud-Mueller, K.-L. Kratz, S. Leenhardt, M. Lewitowicz, C. Longour, M. J. Lopez, F. de Oliveira Santos, L. Petizon, B. Pfeiffer, F. Pougheon, M. G. Saint-Laurent, and J. E. Sauvestre, Nucl. Phys. **A669**, 351 (2000).
[11] R. Grzywacz, R. Béraud, C. Borcea, A. Emsallem, M. Glogowski, H. Grawe, D. Guillemaud-Mueller, M. Hjorth-Jensen, M. Houry, M. Lewitowicz, A. C. Mueller, A. Nowak, A. Płochocki, M. Pfützner, K. Rykaczewski, M. G. Saint-Laurent, J. E. Sauvestre, M. Schaefer, O. Sorlin, J. Szerypo, W. Trinder, S. Viteritti, and J. Winfield, Phys. Rev. Lett. **81**, 766 (1998).
[12] A. M. Nathan, J. W. Olness, E. K. Warburton, and J. B. McGrory, Phys. Rev. C **16**, 192 (1977).
[13] E. K. Warburton, J. W. Olness, A. M. Nathan, J. J. Kolata, and J. B. McGrory, Phys. Rev. C **16**, 1027 (1977).
[14] A. M. Nathan, J. W. Olness, E. K. Warburton, and J. B. McGrory, Phys. Rev. C **17**, 1008 (1978).
[15] E. K. Warburton, J. W. Olness, A. M. Nathan, and A. R. Poletti, Phys. Rev. C **18**, 1637 (1978).
[16] D. E. Appelbe, C. J. Barton, M. H. Muikku, J. Simpson, D. D. Warner, C. W. Beausang, M. A. Caprio, J. R. Cooper, J. R. Novak, N. V. Zamfir, R.A.E. Austin, J. A. Cameron, C. Malcolmson, J. C. Waddington, and F. R. Xu, Phys. Rev. C **67**, 034309 (2003).
[17] A. Gavron, Phys. Rev. C **21**, 230 (1980).
[18] I. Y. Lee, Nucl. Phys. **A520**, 641c (1990).
[19] C. N. Davids, B. B. Back, K. Bindra, D. J. Henderson, W. Kutschera, T. Lauritsen, Y. Nagame, P. Sugathan, A. V. Ramayya, and W. B. Walters, Nucl. Instrum. Methods Phys. Res. B **70**, 358 (1992).
[20] A. N. James, T. P. Morrison, K. L. Ying, K. A. Connell, H. G. Price, and J. Simpson, Nucl. Instrum. Methods Phys. Res. A **267**, 144 (1988).
[21] D. E. Appelbe, G. Martinez-Pinedo, R.A.E. Austin, J. A. Cameron, J. Chenkin, T. E. Drake, B. Djerroud, S. Flibotte, D. N. Parker, C. E. Svensson, J. C. Waddington, and D. Ward, Phys. Rev. C **62**, 064314 (2000).
[22] U. Bosch, W.-D. Schmidt-Ott, E. Runte, P. Tidemand-Petersson, P. Koschel, F. Meissner, R. Kirchner, O. Klepper, E. Roeckl, K. Rykaczewski, and D. Schardt, Nucl. Phys. **A477**, 89 (1988).
[23] S. J. Freeman *et al.* (to be published).
[24] M. Oinonen, U. Köster, J. Äystö, V. Fedoseyev, V. Mishin, J. Huikari, A. Jokinen, A. Nieminen, K. Peräjärvi, A. Knipper, and G. Walter, Eur. J. Phys. **10**, 123 (2001).
[25] R. D. Lawson, *Theory of the Nuclear Shell Model* (Oxford University Press, Oxford, 1980).
[26] W. Nazarewicz, J. Dudek, R. Bengtsson, and I. Ragnarsson, Nucl. Phys. **A435**, 397 (1985).
[27] E. Bouchez, I. Matea, W. Korten, F. Becker, B. Blank, C. Borcea, A. Buta, A. Emsallem, G. de France, J. Genevey, F. Hannachi, K. Hauschild, A. Hürstel, Y. Le Coz, M. Lewitowicz, R. Lucas, F. Negoita, F. de Oliveira Santos, D. Pantelica, J. Pinston, P. Rahkila, M. Rejmund, M. Stanoiu, and Ch. Theisen, Phys. Rev. Lett. **90**, 082502 (2003).
[28] P. F. Mantica, A. C. Morton, B. A. Brown, A. D. Davies, T. Glasmacher, D. E. Groh, S. N. Liddick, D. J. Morrissey, W. F. Mueller, H. Schatz, A. Stolz, S. L. Tabor, M. Honma, M. Horoi, and T. Otsuka, Phys. Rev. C **67**, 014311 (2003).